# Cluster calorimetry by femtosecond stimulated emission pumping: Excitation and evaporative cooling of $I_2^-(CO_2)_n$

R. Wester, A. V. Davis, A. E. Bragg, and D. M. Neumark*

*Department of Chemistry, University of California Berkeley, Berkeley, California, 94720*
(Received 13 November 2001; published 22 April 2002)

Femtosecond stimulated emission pumping has been employed as a technique to prepare small clusters with well-known amounts of internal excitation. In this way $I_2^-(CO_2)_{4,5}$ clusters are prepared with 0.58 to 0.99 eV of internal energy. Subsequent evaporation of between two and four $CO_2$ monomers from the primary cluster is observed as a function of excitation energy using tandem time-of-flight mass spectrometry. Analysis of the appearance energies of the open channels using phase-space theory and photoelectron spectroscopy data yields binding energies of the first eight $CO_2$ molecules to $I_2^-(CO_2)_n$ clusters.

The study of clusters in which a solute is surrounded by a known number of solvent species offers a unique opportunity to probe how the properties of an isolated atom or molecule evolve upon stepwise solvation, with sufficiently large clusters mimicking a condensed phase environment for the solute. An increasingly sophisticated array of spectroscopic and dynamics techniques have been applied to neutral and ionic clusters of this type [1,2]. However, the detailed interpretation of many of these experiments is hampered by lack of knowledge of the basic thermodynamics of the cluster, in particular the binding energies of the individual solvent species. In this paper, we describe an experimental technique in which femtosecond stimulated emission pumping (FSEP) deposits a known and variable amount of vibrational energy into the $I_2^-$ chromophore of $I_2^-(CO_2)_n$ clusters. One can then perform "cluster calorimetry" by monitoring the extent of $CO_2$ evaporation as a function of excitation energy, thereby determining the binding energy of each $CO_2$ molecule.

$I_2^-(CO_2)_n$ clusters provide a rich model system for understanding how a simple gas phase reaction, the photodissociation of $I_2^-$, is altered when the $I_2^-$ chromophore is embedded in a cluster [3,4]. Excitation of the $\tilde{A}'^2\Pi_{g,1/2} \leftarrow \tilde{X}^2\Sigma_u^+$ transition (see Fig. 1) in bare $I_2^-$ yields $I + I^-$ with unit efficiency, but Papanikolas et al. and Vorsa et al. [5,6] demonstrated that in clusters with six or more $CO_2$ molecules, some or all of the recoiling photofragments are "caged" by the surrounding solvent molecules and recombine to form $I_2^-$ that eventually relaxes to the bottom of the $\tilde{X}^2\Sigma_u^+$ state well, a process similar to geminate recombination in solution [7]. In the clusters, highly excited $I_2^-$ formed by recombination transfers vibrational energy to the surrounding $CO_2$ molecules that are eventually ejected from the cluster (evaporative cooling). Excitation at 720 nm (1.75 eV) results in the loss of 7 $CO_2$ molecules from clusters with $10 < n < 22$, yielding an average binding energy of 0.25 eV [5]; this value is an upper bound because each $CO_2$ molecule leaves with nonzero kinetic energy.

The FSEP experiment described herein provides a more precise means of determining cluster binding energies and is applied to the clusters $I_2^-(CO_2)_n (n=4,5)$. The principle of this technique is shown in Fig. 1. A femtosecond pump pulse initiates dissociation of the $I_2^-$ chromophore on the repulsive $\tilde{A}'^2\Pi_{g,1/2}$ state, while an appropriately delayed femtosecond dump pulse transfers a portion of the dissociating wave packet back to the $\tilde{X}^2\Sigma_u^+$ state. The excitation energy of the resulting vibrational wave packet is given by $h\nu_{pump} - h\nu_{dump}$ and is controlled by tuning the energy of the dump photon. In previous experiments on $I_2^-$ and $I_2^-(CO_2)_4$ [8,9], the short-time dynamics of the wave packet created by FSEP were probed by photodetachment with a third femtosecond laser and measurement of the resulting photoelectron spectrum as a function of dump-probe delay. The work on $I_2^-(CO_2)_4$ showed that the vibrationally excited $I_2^-$ relaxes on a time scale of 4 ps, transferring its energy to the surrounding solvent molecules [9]. Here, we examine the dynamics in these excited clusters on a much longer time scale,
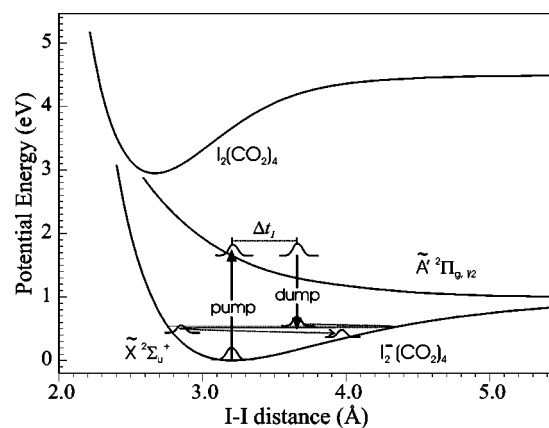


FIG. 1. Potential energy curves along the $I_2$ internuclear bond distance relevant to FSEP in $I_2^-(CO_2)_4$. The $\tilde{X}^2\Sigma_u^+$ and $\tilde{A}'^2\Pi_{g,1/2}$ for $I_2^-$ are shown [10,11], shifted appropriately with respect to the ground state of neutral $I_2(CO_2)_4$. Stimulated emission pumping using pump and dump pulses (vertical arrows) leads to the formation of an excited wave packet with energy $h\nu_{pump} - h\nu_{dump}$ that subsequently loses energy to the cluster.

*Author to whom correspondence may be addressed. Email address: dan@radon.cchem.berkeley.edu

R. WESTER, A. V. DAVIS, A. E. BRAGG, AND D. M. NEUMARK

using photofragment mass spectrometry to determine the extent of fragmentation several microseconds after the dump pulse. While this experiment is not time resolved per se, femtosecond pump and dump pulses are needed so that SEP can compete with rapid dissociation ($\sim 300$ fs [10]) on the $\tilde{A}'\,^2\Pi_{g,1/2}$ state.

In the instrument, described in detail elsewhere [12], $I_2^-(CO_2)_n$ clusters are produced by passing argon carrier gas admixed with 2.5% $CO_2$ over crystalline iodine and expanding it into vacuum through a pulsed nozzle. The expansion is crossed with a 1.2 keV electron beam, producing $I_2^-(CO_2)_n$ clusters. The clusters are mass separated using a Wiley-McLaren time-of-flight (TOF) mass spectrometer. The temporal mass focus of the Wiley-McLaren field configuration occurs at the interaction point with the femtosecond laser pulses. A high-voltage mass gate is used to block all anions except those of the desired mass. The repetition frequency of the pulsed ion source is 500 Hz, matching that of the laser.

The femtosecond laser system (Clark MXR) produces 80 fs pulses centered at 790 nm (1.57 eV). The pulses are split, with 70 $\mu$J of the pulse energy used for the pump beam, while 400 $\mu$J pulses pump an optical parametric amplifier (TOPAS) to produce tunable dump pulses with 1150 to 1850 nm center wavelength (1.08 to 0.67 eV) and between 20 and 60 $\mu$J pulse energy. The 790 nm pump pulse and the tunable dump pulse are made collinear and focused to a 1 mm diameter spot at the ion-beam interaction region. The time delay between the pump and dump pulses, $\sim 100$ fs, is controlled by an optical delay stage. Both pulses are delayed appropriately with respect to the pulsed ion source in order to intercept the anion packet of the desired mass.

Fragmentation of the primary $I_2^-(CO_2)_{4,5}$ clusters results from photodissociation by the pump beam alone and by evaporation of $CO_2$ molecules due to excitation by stimulated emission pumping. The mass spectrum of the photofragments is obtained using a reflectron TOF mass analyzer downstream of the laser interaction region; the flight time from the interaction region to the reflectron is $\sim 30$ $\mu$s. After being reflected in the constant electric field of the reflectron, the photofragments are detected with a microchannel plate (MCP) detector. Their flight times are determined by feeding the MCP pulses through a fast preamplifier and into a multichannel scaler (Stanford Research Systems SR430). Background subtraction was performed in the multichannel scaler on a shot-to-shot basis using a synchronized chopper wheel that blocked every other laser pulse. In this way, reflectron TOF spectra were acquired over $10^4$ to $10^5$ laser shots. All measurements were repeated at several electric-field strengths in the reflectron, corresponding to different ion trajectories; while the peak shapes changed due to different temporal focusing, the relative peak intensities were not altered significantly.

Photofragment mass spectra were obtained for eight different dump wavelengths, corresponding to $I_2^-$ excitation energies between 0.48 and 0.89 eV, or 47 to 88 % of the $I_2^-$ dissociation energy of 1.01 eV [11]. In addition, fragment spectra were recorded with the pump beam only. The energy resolution of the excitation process is 30 meV, determined by
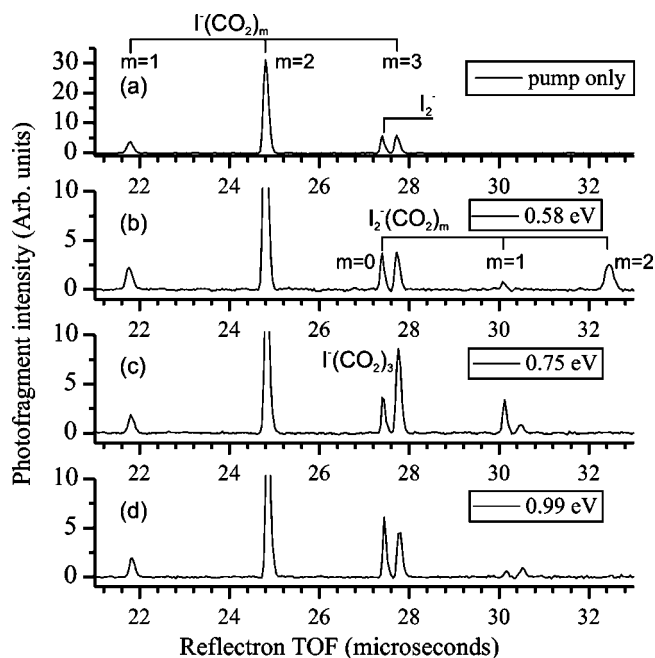


FIG. 2. Reflectron time-of-flight photofragment mass spectra for $I_2^-(CO_2)_4$; (a) pump only, (b)–(d) after stimulated emission pumping at three different excitation energies (including the initial internal energy $E_{int} = 100$ meV) leading to additional $I_2^-(CO_2)_m$ fragments after $CO_2$ evaporation.

the bandwidth of the femtosecond pulses. The internal energy of the clusters produced by the ion source is estimated to be $E_{int} = (100 \pm 50)$ meV, based on vibrational hot band intensities in the photoelectron spectra of $I_2^-(CO_2)_n$ [13], and this energy must be added to the excitation from the pump and dump pulses since it is available for solvent evaporation. The $I_2^-(CO_2)_{4,5}$ clusters are therefore prepared with excitation energies ranging from $E_{ex} = 0.58$ to 0.99 eV.

Figs. 2(a)–2(d) shows representative photofragment mass spectra of $I_2^-(CO_2)_4$ using the pump laser only and for three different cluster excitation energies $E_{ex}$. Excitation with the pump beam alone yields predominantly $I^-(CO_2)_m$ fragments, indicating successful photodissociation of the $I_2^-$ chromophore. A small amount of bare $I_2^-$ is observed due to cluster-induced recombination followed by evaporation of all the $CO_2$ molecules, in agreement with earlier experiments by Vorsa et al. [14]. Figures 2(b)–2(d), at $E_{ex} = 0.58$, 0.75, and 0.99 eV, respectively, show additional $I_2^-(CO_2)_m$ cluster peaks, a result of the dump pulse driving some of the dissociating $I_2^-$ back to its ground electronic state. Energy transfer from the vibrationally excited $I_2^-$ to the $CO_2$ molecules leads to $CO_2$ evaporation giving rise to $I_2^-(CO_2)_m$ mass peaks with $m < 4$. The number of evaporated $CO_2$ molecules increases with excitation energy: for $E_{ex} = 0.58$ eV $I_2^-(CO_2)_2$ is the dominant product channel, whereas for $E_{ex} = 0.75$ eV this peak has vanished and $I_2^-(CO_2)_1$ is the dominant product. At $E_{ex} = 0.99$ eV, the intensity of the $I_2^-(CO_2)_1$ peak has decreased and bare $I_2^-$ is the dominant product.

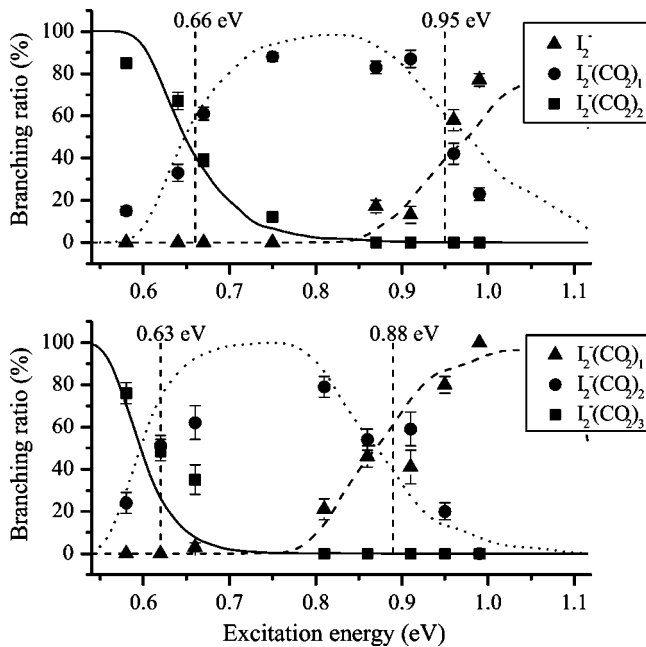Close inspection reveals that the intensity of the

FIG. 3. Photofragment branching ratios as a function of excitation energy indicating the number of $CO_2$ monomers evaporating from the excited parent $I_2^-(CO_2)_4$ (upper panel) and $I_2^-(CO_2)_5$ (lower panel) clusters after stimulated emission pumping. The fitted model based on phase-space theory is given by the solid, dashed, and dotted lines for evaporation of two, three, and four $CO_2$ molecules, respectively.

$I^-(CO_2)_3$ peak increases at $E_{ex}=0.75$ eV. This effect is tentatively attributed to the absorption of a dump photon to a higher excited state of $I_2^-$ correlated to $I^- + I^*(^2P_{1/2})$, rather than stimulated emission back to the $I_2^-$ ground state.

Figure 3 shows the relative intensities of the $I_2^-(CO_2)_m$ peaks from $I_2^-(CO_2)_4$ and $I_2^-(CO_2)_5$ at all eight excitation energies. The error bars are derived from the standard deviations of six individual mass spectra taken at each excitation energy. For both parent clusters, evaporation of two $CO_2$ units is the dominant channel at $E_{ex}=0.58$ eV. As $E_{ex}$ is raised, evaporation of three $CO_2$ molecules becomes favored, and above $\sim 0.95$ eV four $CO_2$ monomers are lost from the parent clusters. Vertical dashed lines in Fig. 3 indicate the excitation energies at which the dominant product channel changes from evaporation of two to three or three to four $CO_2$ molecules.

These crossover points alone cannot be used to extract binding energies. At first glance, one might infer from the $I_2^-(CO_2)_4$ results in Fig. 3(a) that the sum of the binding

energies for the first three ejected $CO_2$'s is 0.66 eV, while the binding energy of the last $CO_2$ is $0.95-0.66=0.29$ eV. This interpretation is incorrect because each $CO_2$ is expected to leave with nonzero kinetic and internal energy, thereby reducing the available energy in the daughter cluster by more than the binding energy [15]. This additional energy loss must be modeled in order to extract quantitative $CO_2$ binding energies from the crossover points.

In order to account for this effect, the measured branching ratios are compared with a theoretical model based on phase-space theory (PST) [16,17] using the binding energies as parameters. Its key element is the distribution $P(\epsilon|n,E)$, the probability for evaporation of a $CO_2$ monomer with total kinetic and internal (vibrational plus rotational) energy $\epsilon$ from an $I_2^-(CO_2)_n$ cluster with internal energy $E$, leaving a daughter ion with internal energy $E-\epsilon$. $P(\epsilon|n,E)$ distributions are calculated using PST, assuming equal flux into all open final states; this is a suitable model for ion cluster dissociation in which no reverse barrier is expected [18,19]. The product vibrational density of states is calculated with the Beyer-Swinehart state counting algorithm, using the known vibrational frequencies of $CO_2$ and cluster mode frequencies taken from electronic structure calculations [13]. The product branching ratios are calculated using a Monte Carlo algorithm that samples the photofragments for an ensemble of primary clusters with given initial excitation. It treats cluster fragmentation as stepwise evaporation of $CO_2$ monomers, each carrying a random kinetic-energy release $\epsilon$ weighted by $P(\epsilon|n,E)$, until the energy of the fragment cluster is smaller than the binding energy of the remaining $CO_2$ monomers. Finally, the calculated branching ratios are convoluted with the experimental energy resolution of 30 meV.

The data are insufficient for an independent determination of the binding energies of the first five $CO_2$ molecules to $I_2^-$. Instead, these binding energies are constrained by using recent results from the photoelectron spectroscopy of $I_2^-(CO_2)_n$ clusters ($n\leqslant 8$) [13]. The photoelectron spectra yield the electron affinity ($E_a$) for each $I_2(CO_2)_n$ cluster. $E_a$ is related to the anion and neutral cluster solvent binding energies by $E_a(n)=E_a(I_2)+\Sigma_{j=1}^n(S_j^{(-)}-S_j^{(0)})$, where $S_j^{(-)}$ and $S_j^{(0)}$ are the (unknown) binding energies of $CO_2$ to $I_2^-(CO_2)_{j-1}$ and $I_2(CO_2)_{j-1}$, respectively. The electron affinities increase with $n$ because the anion binding energies are significantly stronger than the neutral binding energies. In Table I, values are reported for

$$\Delta E_a(n)=E_a(n)-E_a(n-1)=S_n^{(-)}-S_n^{(0)}. \qquad (1)$$

TABLE I. Differences in electron affinity $\Delta E_a(n)$ deduced from photoelectron spectroscopy [13] and derived anion solvent binding energies $S_n^{(-)}$ for $I_2^-(CO_2)_n$ clusters using a one-parameter fit. All energies are in meV. Estimated uncertainties are $\pm 14$ meV for $\Delta E_a(n)$ and $\pm 21$ meV for the anion binding energies $S_n^{(-)}$.

| $n$ | 0 | 1 | 2 | 3 | 4 | 5 | 6 | 7 | 8 |
|---|---|---|---|---|---|---|---|---|---|
| $\Delta E_a(n)$ | 0 | 139 | 111 | 95 | 80 | 75 | 80 | 82 | 83 |
| $S_n^{(-)}$ | 0 | 234 | 206 | 190 | 175 | 170 | 175 | 177 | 178 |

We now assume that all the neutral binding energies are the same, i.e., $S_n^{(0)} = S^{(0)}$, so that the variations in Table I, are due to differences in the anion binding energies. This assumption is based on our expectation that all interactions in the neutral cluster are weaker than in the anion cluster, so that any variations in $S_n^{(0)}$ should be considerably smaller than in $S_n^{(-)}$. $S^{(0)}$ is then the only free parameter in the PST model used to fit the data, because the anion binding energies are all fixed by Eq. (1).

The best-fit fragment branching ratios are shown in Fig. 3 as lines superimposed on the data. We find $S^{(0)} = 95$ meV, yielding values of $S_n^{(-)}$ that decrease from 234 meV for the first $CO_2$ to 170 meV for the fifth $CO_2$, followed by a small increase up to 178 meV for the eighth $CO_2$ (see Table I). The uncertainty of the neutral binding energy $S^{(0)}$ is estimated to be 16 meV, deduced from the $\chi^2$ fit and the uncertainty of the initial internal excitation. This leads to an overall uncertainty of the anion binding energies $S_n^{(-)}$ of $\pm 21$ meV, based on the uncertainty for the electron affinity differences $\Delta E_a(n)$ of $\pm 14$ meV [13].

Our binding energies are significantly lower than the average binding energy of 250 meV per $CO_2$ obtained by Papanikolas et al. [5] in the size range $10 < n < 22$, but, as mentioned earlier, this value is an upper bound because fragment kinetic and internal energy was not considered. They are $\sim 70$ meV lower than the energies calculated by Amar and Perera [20], and lie in the range of those calculated by Papanikolas et al. [21], who found an average binding energy of 190 meV for clusters with $3 < n < 10$. We can also compare our results to those obtained for pure ionic $CO_2$ clusters. Photodissociation experiments by Alexander et al. on $(CO_2)_n^+ (n < 40)$ [22] and $(CO_2)_n^- (13 < n < 26)$ clusters [23] yielded average binding energies of 210 and 220 meV, respectively, which were not corrected for kinetic-energy release. This correction was later performed for $(CO_2)_n^+$ and a binding energy of $156 \pm 26$ meV was obtained [15], in reasonable agreement with our $S_n^{(-)}$ values for $n > 4$ in the mixed anion clusters.

In summary, we have performed "cluster calorimetry" experiments in which femtosecond stimulated emission pumping is used to deposit controlled amounts of internal energy into clusters comprised of solvent species bound to an ionic chromophore. A wide range of excitation energies is possible, and by combining FSEP with photofragment mass spectrometry, one can determine the binding energy of each solvent molecule to the cluster by measuring the extent of solvent evaporation as a function of excitation energy. This technique can be readily extended to other solvent species, such as Ar or $H_2O$, surrounding a chromophore ion, and represents a means of determining solvent binding energies in clusters.

[1] A.W. Castleman and K.H. Bowen, J. Phys. Chem. **100**, 12 911 (1996).

[2] M.A. Duncan, Int. J. Mass. Spectrom. **200**, 545 (2000).

[3] R. Parson, J. Faeder, and N. Delaney, J. Phys. Chem. A **104**, 9653 (2000).

[4] C.J. Margulis and D.F. Coker, J. Chem. Phys. **110**, 5677 (1999).

[5] J.M. Papanikolas, et al., J. Phys. Chem. **95**, 8028 (1991).

[6] V. Vorsa, et al., J. Chem. Phys. **106**, 1402 (1997).

[7] A.L. Harris, J.K. Brown, and C.B. Harris, Annu. Rev. Phys. Chem. **39**, 341 (1988).

[8] M.T. Zanni, et al., J. Chem. Phys. **112**, 8847 (2000).

[9] A.V. Davis, et al., J. Electron Spectrosc. Relat. Phenom. **112**, 221 (2000).

[10] M.T. Zanni, et al., J. Chem. Phys. **110**, 3748 (1999).

[11] M.T. Zanni, et al., J. Chem. Phys. **107**, 7613 (1997).

[12] B.J. Greenblatt, M.T. Zanni, and D.M. Neumark, Faraday Discuss. **108**, 101 (1998).

[13] H. Gomez, T. R. Taylor, and D. M. Neumark J. Phys. Chem. A (to be published).

[14] V. Vorsa, et al., J. Chem. Phys. **105**, 2298 (1996).

[15] P.C. Engelking, J. Chem. Phys. **85**, 3103 (1986).

[16] P. Pechukas and J.C. Light, J. Chem. Phys. **42**, 3281 (1965).

[17] P. Pechukas, J.C. Light, and C. Rankin, J. Chem. Phys. **44**, 794 (1966).

[18] C.E. Klots, J. Phys. Chem. **75**, 1526 (1971).

[19] W.J. Chesnavich and M.T. Bowers, J. Chem. Phys. **66**, 2306 (1977).

[20] F.G. Amar and L. Perera, Z. Phys. D: At., Mol. Clusters **20**, 173 (1991).

[21] J.M. Papanikolas, P.E. Maslen, and R. Parson, J. Chem. Phys. **102**, 2452 (1995).

[22] M.L. Alexander, M.A. Johnson, and W.C. Lineberger, J. Chem. Phys. **82**, 5288 (1985).

[23] M.L. Alexander, M.A. Johnson, N.E. Levinger, and W.C. Lineberger, Phys. Rev. Lett. **57**, 976 (1985).